Synergistic Sorption of Tartrazine Dye: Exploring the Combined Potential of Kaolinite and Zinc Oxide Composite in Wastewater Treatment

[*1]Egah, G.O., [2]Sha'Ato, R., [2]Itodo, A.U and [2]Wuana, R.A

[1]*Chemical Sciences Department, Faculty of Pure and Applied Sciences, Federal university Wukari, Taraba State, Nigeria*
[2]*Chemistry Department, Faculty of Physical Sciences, Joseph Sarwuan Tarka University (Formerly Federal University of Agriculture) Makurdi Benue State, Nigeria*
Corresponding email: egah.godwin@yahoo.com

ABSTRACT

Background: *Textile and plastic industries are major sources of tartrazine dye. In industries, dyes are used as colorants in their industrial processes. Tartrazine dye has been reported to cause harm even at trace levels.*

Material and Methods: *This study compared the adsorption of tartrazine dye on raw kaolinite (RK) and kaolinite–zinc oxide composite (KZC). These adsorbent features were determined using X-ray fluorescence (XRF) to determine adsorbent chemical composition, Fourier transformed infrared spectroscopy (FTIR) for functional groups, Scanning electron microscope (SEM) techniques, and Brunauer-Emmett-Teller (BET) was used to determine the structural morphology, surface area respectively. The batch experiment was conducted for the effect of pH at the range of (3 -11), initial tartrazine concentration of (50 - 250 mg/L), adsorbent dose of (0.5 - 2.5 g), contact time (10 - 60 min) and temperature (298 - 328 K) were evaluated.*

Results: *The RK and KZC showed the following physicochemical properties: pH 6.03 and 5.12; pHzpc: 6.80 and 6.00 for RK and KZC respectively; Conductivity (20μS/cm): 88.30 and 68.20; Bulky density (g/cm^3): 1.191 and 1.000; Attrition (%):12.00 and 12.00; Iodine number: 825.3 and 780.6 respectively. Adsorbent RK and KZC were found to have a surface area of 355.744 (m^2/g) and 385.734 (m^2/g) respectively. Pore sizes of 2 - 6 nm were found and classified as meso-pores.*

Conclusion: *As investigated, the adsorption capacity of tartrazine was favored by an increase in dosage, solution concentrations, and contact time. While an increase in temperature decreases their percentage removal. The optimum pH for the adsorption of tartrazine was found to be 3. The experimental data of tartrazine fitted better into the linearized D-R and Freundlich isotherm than Langmuir isotherm indicating multilayer adsorption. Kinetic data fitted more into pseudo second order than first order and intra-particle diffusion model suggesting chemisorption as the rate limiting step. For the calculated thermodynamic parameters, the negative values of enthalpy change, entropy change, and Gibbs free energy indicated that the adsorption of tartrazine was exothermic and spontaneous, meaning that physisorption dominates chemisorption. In comparison of RK and KZC, as investigated in the present study, it is evident that the composites KZC have a higher percentage removal of 96.3065 % than the RK with 94.6075 %. The Duncan test for Tartrazine shows that the means of KZC is significantly greater than that of RK suggesting KZC composite to be more potent than RK adsorbent.*

Keywords: Tartrazine, Kaolinite, Adsorption, Isotherm and Thermodynamics

---
Date of Submission: 01-03-2024   Date of Acceptance: 10-03-2024

I. INTRODUCTION

Increases in industrial activities have exposed water to pollutants such as azo-dye (Dwivedi, 2017). In industries like textile, food, plastics, pesticide, soap, paint, and pharmaceutical industries, dyes are used as colorants in their industrial processes (Huang *et al.,* 2017; Singh *et al.,* 2019). This makes wastewater from these industries have refractory particles of these dyes (Srivastav *et al.,* 2019). Many dyes are made from carcinogens like benzidine which bio-accumulates in the human system (Ratna and Padhi, 2012). High concentrations of tartrazine in the animal system cause permanent blindness, itching, liver and kidney damage, dysfunction of the nervous system, mental disorders, asthma, decrease in RBC count (dyscrasia), cancer, hyperactivity, and infertility (Sartape *et al.,* 2017; Prajapati and Mondal, 2020).

Various conventional methods such as coagulation and flocculation, oxidation or zonation, and membrane separation, have been reported for the removal of dyes, but are too expensive and not feasible on an industrial scale (Berez *et al.,* 2014; Srivastav *et al.,* 2019). Therefore, it is pertinent to look for cheap and

efficient treatment methods for the removal of this pollutant from wastewater. Adsorption using raw kaolinite has proven to be a viable method for the removal of refractory pollutants. It is used due to its large surface area, ion exchange, high versatility, and low costs (De-Gisi *et al.,* 2016). This study seeks to use raw kaolinite and compare it with its enhanced synergy of kaolinite - zinc oxide composite using isotherm, kinetic, and thermodynamic study.

II. MATERIALS AND METHODS

Preparation of Adsorbent

Methods of kaolinite-zinc oxide composite (KZC) preparation were adopted from Egah *et al.,* (2019) with little modification. The kaolinite - zinc oxide (KZC) composite was prepared synergistically by mixing kaolinite with zinc-oxide in a 3:1 ratio. The resulting mixture was then calcined at 700 ^{o}C for 1 h and stored for adsorption. The reaction is given in equation (1):

Kaolinite ($Al_2O_3SiO_2H_2O$) + ZnO → ZnO($Al_2O_3SiO_2H_2O$) composite   (1)

Also, the raw kaolinite (RK) used was supplied by Knexel Nigeria Limited, no; 27, Adeleke Street, Ikeja, Lagos State, Nigeria without any modification. The raw kaolinite (RK) was prepared by calcining 2 kg at 600 $^{\circ}$C for 1 h in a muffle furnace to destroy its structure and any undesired volatile matter. It was sieved using a 50 mm mesh sieve on a shaker to determine the particle size and stored as raw adsorbent RK for adsorption (Karapinar and Donat, 2009).

Characterization of the Adsorbent
Physico - chemical characteristics of the adsorbent
The following physiochemical characterizations were carried out for adsorbents RK and KZC.

Determination of adsorbent surface area, pore volume and pore size

BET surface area was determined using methods adopted by Dada *et al.,* (2017). It utilizes probing gases that do not chemically react with material surfaces to quantify specific surface area (Dada *et al.,* 2017). Specific surface areas of the prepared adsorbents were evaluated through N_2 adsorption at 77 K, using an Autosorb1-Quantachrome instrument (NOVA 4200e USA). The BET (Brunauer–Emmett - Teller) model was applied to fit Nitrogen adsorption isotherm and to evaluate the surface area (S_{BET}) of the sorbent. Pore size and pore volume were estimated using Density Functional Theory (DFT). The readings were taken in triplicates to ensure accuracy (Thommes *et al.,* 2015).

Determination of adsorbents iodine number

The adsorbent iodine number was determined according to the ASTM D4607-14 method. Iodine number is defined as the milligrams of iodine adsorbed by 1.0 g of adsorbent when the iodine concentration of the filtrate is 0.02 M (0.02 mol L^{-1}) (Nunes and Guerreiro, 2011). A standard iodine solution was treated with three different weights of adsorbent under specified conditions. 0.5, 1.0, and 1.5 g each of the dry adsorbents were placed in a dry 250 mL Erlenmeyer flask, and 10.0 mL of 5% HCl was added. This mixture was boiled for 30 s to remove sulfur that can interfere with the results. Thereafter, 50.0 mL of 0.1 M (0.1 molL^{-1}) iodine solution was added to the mixture and stirred for 30 seconds. The resultant solution was filtered and 25.0 mL of the filtrate known as gram iodine was pipetted and titrated with 0.1 M (0.1 mol L^{-1}) sodium thiosulfate, using 1 mL starch indicator solution. Starch forms a dark purple complex when added to iodine. The reaction is as given in Equation (2):

$2Na_2S_2O_3 + I_2 \rightarrow Na_2S_4O_6 + 2NaI$ (2)

The iodine number is the Qe/M value when the residual concentration (Ce) is 0.02 M (0.02 molL^{-1}). The Qe/M (Y) and Ce (X) values were calculated by the Equations (3-4):

$$\frac{Q_e}{M} = \frac{\{(M_1 \times 126.93 \times V_1) - [\frac{(V_1 + V_{HCl})}{V_F}] \times (M_{Na_2S_2O_3} \times 126.93) \times V_{Na_2S_2O_3}\}}{M_C}$$ (3)

$$Ce = \frac{M_{Na_2S_2O_3} \times S}{F}$$ (4)

where M_I is the iodine solution molarity, V_I is the added volume of iodine solution, V_{HCl} is the added volume of 5% HCl, V_F is the filtrate volume used in titration, $M_{Na_2S_2O_3}$ is the sodium thiosulfate solution molarity, $V_{Na_2S_2O_3}$ is the consumed volume of sodium thiosulfate solution and M_C is the mass of adsorbent, Ce is the residual filtrate concentration (M), S is the volume sodium thiosulfate consumed, mL and F the volume of filtrate used.

Determination of pH

The pH of the adsorbents and catalyst was determined by the method adopted by Sha'Ato *et al.,* (2018). One gram of the absorbents was weighed into 100 mL distilled water in a beaker and kept on a magnetic stirrer for 1 hr at 120 rpm. The pH was then measured using the stirred slurry using the HI 8014 pH meter (Hanna instruments). To ensure the accuracy and reliability of results, measurements were made in triplicates.

Determination of pH at point of zero charge (pHp$_{ZC}$)

The pH at the Point of zero charge (PZC) is defined as the pH at which the adsorbent surface has a net neutral electrical charge (Dada et al., 2017). The pHzpc was determined by the salt addition method adopted by Pouretedal and Sadegh, (2014). The pHzpc is the point where the curve of pH (final) vs pH (initial) intersects. To determine the pHpzc of the adsorbent, 25 ml of 0.1 M NaCl solution were placed in five different conical flasks and their pH's were adjusted to (2, 4, 7, 8, and 10) with HCl and NaOH and labeled as initial pH's (pH$_{Initial}$). 0.5 g of the adsorbents were added to each and shaken for 2 hrs. The suspension was then filtered and the filtrate was measured as pH$_{Final}$. A plot of pH$_{Initial}$ on the X-axis and pH$_{Final}$ − pH$_{Initial}$ on the Y-axis gives an intercept on the X-axis referred to as the pH at the point of zero charge (Dada *et al.,* 2017).

Conductivity (μS/cm) of adsorbents

Conductivity was measured using the method reported by Sha'Ato *et al.,* (2018). One gram sample of the adsorbent was added to 100 mL distilled water and stirred for 20 minutes and its conductivity was measured in two micro-Siemen (2μS/cm) using a DDS-307 conductivity meter (Pec Medicals USA) in triplicate.

Bulk density of adsorbents

The bulk density was determined using the tamping method adopted by Egah *et al.,* (2019). 5 g of each adsorbent was packed in a 10 mL measuring cylinder separately and tamped until it occupied a minimum volume. The apparent volumes were read as the differences between the initial and the final volumes. The bulk density results were taken in triplicates to ensure the reliability of the results. The bulk density was calculated as in Equation (5):

$$Bulk\ density\ (g/cm^3) = \frac{Mass\ of\ the\ adsorbent\ (g)}{Apparent\ Volume\ of\ adsorbent\ (cm^3)} \qquad (5)$$

Percentage attrition/hardness

Attrition or hardness is the measure of mechanical strength and it is an important parameter used to determine the adsorbent's ability to withstand normal handling operations. The attrition of the samples was measured using the wet attrition method described by Sha'Ato *et al.,* (2018). One gram sample of the adsorbent was added to 100 mL of distilled water and stirred at 200 rpm for 2 hrs using a magnetic stirrer. The solution was then filtered using filter paper and the residue dried at room temperature. The % attrition was calculated as in Equation (6):

$$Attrition\ (\%) = \frac{Initial\ mass(g) - Final\ mass(g)}{Initial\ mass(g)} \times 100 \qquad (6)$$

Instrumental Characterization of Adsorbents
Scanning electron microscopy (SEM) analysis

Scanning electron microscopy (SEM) was used to determine the surface structure and shape of an adsorbent (Naswir *et al.,* 2013). The SEM imaging was carried out at a multidisciplinary central laboratory, at the University of Ibadan, Oyo State. A scanning electron microscope (SEM - JEOL, JSM 7600 F) was used to determine the surface texture and porosity of the adsorbent and catalyst. A thin layer of platinum was sputter-coated on the adsorbent for charge dissipation during SEM imaging. The sputter coater (Eiko IB-5 Sputter Coater) was operated in an argon atmosphere using a current of 6 mA for 3 min. The coated samples were then transferred to the SEM specimen chamber and observed at an accelerating voltage of 5 kV, eight spot size, four apertures, and 15 mm working distance (Egah *et al.,* 2023).

Fourier transformed infra-red (FTIR) analysis

The FT-IR was carried out at the multidisciplinary Central Laboratory, University of Ibadan, Oyo State. This method of analysis was conducted to determine the existence of the surface functional groups of the adsorbent. The Fourier transform infrared (FTIR) spectra were collected in the range of 350-4400 cm^{-1} using the KBr disk method (Johari *et al.,* 2014).

X-ray fluorescence (XRF) analysis
The XRF analyses were carried out at the Engineering Materials Development Institute, Akure, Ondo State. Sky-ray Instrument (EDX3600B X-ray fluorescence) was used. This method of analysis will be used to determine the chemical composition of the adsorbents. The samples were pulverized to fine homogeneous size and then pelletized before analysis.

Stock Preparation of Tartrazine Solutions
Methods of adsorbate preparation were adopted from Makeswari *et al., (*2016). The stock solution of 500 mg/L was prepared by dissolving 0.5 g of analytical-grade tartrazine in a 1-liter volumetric flask and made up to the mark with deionized water. Several standard concentrations of tartrazine (50, 100, 150, 200, 250 mg/L) were prepared from the stock solution by serial dilution. The Tartrazine adsorbate (I), trisodium-5-hydroxy-1-(4-sulfonate phenyl)-4-(4-sulfonate-phenyl azo)-H-pyrazole-3carboxylate is an azodye with molecular formula of $C_{16}H_9N_4Na_3O_9S_2$ (Figure 1), molecular mass of 534.36 (gmol^{-1}) and wavelength (λmax 426 (nm).
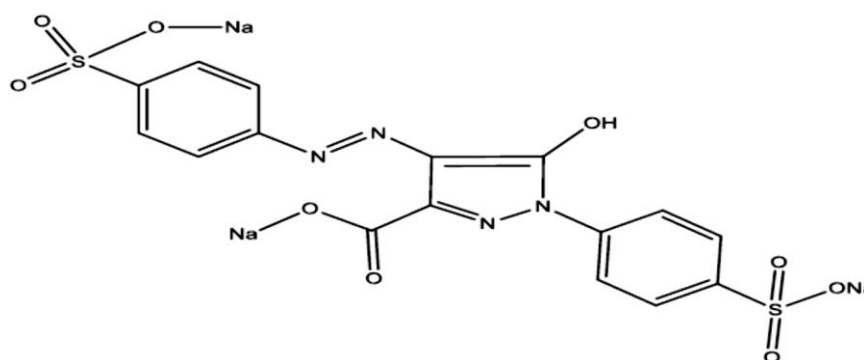

Figure 1: Structure of Tartrazine

Batch Adsorption Experiments
Batch experiments were carried out according to methods adopted by Sha'Ato *et al., (*2018). Bath experiments were conducted for all the adsorbents RK and KZC at room temperature of 298 K. The effect of pH (3, 5, 7, 9 and 11), initial tartrazine concentration of (50, 100, 150, 200 and 250 mg/L), adsorbent dose (0.5, 1.0, 1.5, 2.0, and 2.5 g), contact time (10, 20, 30, 40 and 60 min) and temperature (298, 308, 318 and 328 K) were evaluated. In the batch experiment, 0.5 g of each adsorbent was contacted with 50 mL of 50 mg/L adsorbate solution in a conical flask (250 mL) in capacity, and stirred for (60 minutes) constant contact time by mechanical shaker at (200 rpm) at room temperature until equilibrium is achieved. At the end of the contact time required, the solution were centrifuged and filtered using whatman No. 1 filtered paper, and the filtrate analyzed for residual concentrations of tartrazine using UV-visible spectrophotometer (Shimadzu, UV-1700 spectrophotometer) at a maximum wavelength of 426 (Dong *et al.,* 2010). In all batch adsorption experiments, the amount Q_e (mg/g), is calculated using the mass balance Equation (7) adopted by Kibami *et al.,* (2014):

$$Q_{e\ (mg/g)} = \frac{(C_o - C_e)}{M_a} v \qquad (7)$$

where Q_e represent the adsorption capacity, C_o and C_e are the initial and residual concentrations (mg/L), respectively; *V* will be the aliquot volume of solution in (L) or dm^3 used and m_a the mass of adsorbent in (g) used for a particular batch treatment.
The percentage removal of the adsorbate is calculated as Equation (8):

$$\%\ Removal = \frac{(C_o - C_e)}{C_o} \times 100 \qquad (8)$$

Adsorption Isotherms
In this research, the Langmuir, Freundlich and Dubinin-Radushkevich adsorption isotherms models was used in this study.

Langmuir adsorption isotherm
The Langmuir equation is based on assumptions, that the adsorbent surface is homogeneous and all sites are equivalent having constant and equivalent heat of adsorption for all sites and monolayer adsorption occurs only on the adsorbent surface (Al-Ghouti and Da'ana, 2020). According to Asiagwu *et al.* (2018), the linear Langmuir adsorption isotherm is expressed as Equation (9):

$$\frac{1}{Q_e} = \frac{1}{Q_m} + \frac{1}{C_e} \times \frac{1}{bQ_m} \qquad (9)$$

where Q_m (mg/g) is the monolayer sorption capacity at equilibrium for the Adsorbate-Adsorbent which is the total number of binding sites that are available for sorption, C_e is the equilibrium concentration of the solute in the bulk solution (mg/L), Q_e (mg/g) is the amount of solute sorbed per unit mass of the adsorbent at equilibrium which is the number of binding sites that are in fact occupied by the sorbate at the final or equilibrium concentration and b (L/mg) is the Langmuir constant for the adsorbate-adsorbent. The magnitude of b expresses the affinity between the adsorbent and adsorbate which is largely determined by the heat of sorption. The higher the magnitude of b, the higher the heat of sorption and the stronger the bond formed (Egah *et al.*, 2023). A linear plot of $1/Q_e$ versus $1/C_e$ gives a straight line, with the slope and the intercept of $1/Q_m$ and $1/bQ_m$. The characteristics of the Langmuir isotherm are determined by the dimensionless constant called separation factor, R_L expressed as Equation (10):

$$R_L = \frac{1}{(1+bc_0)} \qquad (10)$$

where b (L/mg) is the Langmuir constant for adsorbate-adsorbent and C_0 (mg/L) the initial adsorbate concentration. R_L indicates the nature of adsorption process shown as: $R_L > 1$, is unfavourable, $R_L = 1$ is linear, R_L between 0 - 1 is favourable and $R_L = 0$ is irreversible (Sha'Ato *et al.,* 2018).

Freundlich adsorption isotherm

The Freundlich adsorption equation is perhaps the most widely used mathematical description of adsorption in aqueous systems. The Freundlich isotherm is based on multilayer adsorption on the heterogeneous surface of the adsorbent obtaining an unequal amount of energy (Okeola *et al.,* 2017). It is not limited to monolayer adsorption, but also it is applied to multi-layer adsorption. The linear equation of Freundlich adsorption isotherm as adopted by Egah *et al.,* (2023) is given as Equation (11):

$$logQ_e = \frac{1}{n}logc_e + logK_f \qquad (11)$$

where Qe (mg/g) is the amount of adsorbate that is adsorbed per unit mass of the adsorbent and Ce (mg/L) is the equilibrium concentration. K_F is the Freundlich constant related to the adsorption capacity and 1/n is a function of the strength of adsorption, which varies with the heterogeneity of the material (Egah *et al.,* 2019) When n = 1, the boundary between the two phases is independent of the concentration. 1/n below 1 indicates a normal adsorption. A linear plot of log Qe versus log Ce, gives the slope of n and intercept K_F. If the value of n lies in the range of 1 - 10, they are classified as favorable adsorption according to Freundlich as reported by Sha'Ato et al. (2018).

Dubinin-radushkevich (D-R) isotherm

Dubinin and his co-workers conceived this equation for micropore solids. D-R isotherm helps to determine the adsorption mechanism. It distinguished between the chemical adsorption and physical adsorption. The linear form of the D-R Equation as adopted by Al-Ghouti and Da'ana, (2020) is given as Equation (12):

$$Inq_e = lnq_m - K\varepsilon^2 \qquad (12)$$

where, Q_e = amount of adsorbate adsorbed per unit weight of adsorbent at equilibrium (mgg^{-1}), Q_m = Maximum adsorption capacity of adsorbent (mgg^{-1}), K = constant related to adsorption energy, ε = polanyi potential (kJ^{2}mol^{-2}). The Polanyi potential ε can be acquired from equation (13)

$$\varepsilon = RTln(1 + \frac{1}{C_e}) \qquad (13)$$

where, R is gas constant, T is the temperature in (K), Ce is the concentration of adsorbate at equilibrium in solution after adsorption (mgL^{-1}). The experimental data was evaluated by plotting lnQe against ε^2. The values of Q_m and K are estimated from the intercept and slope respectively. The mean adsorption energy is calculated with the Equation (14):

$$\varepsilon = \frac{1}{\sqrt{2K}} \qquad (14)$$

As reported by Nwodika and Onukwuli, (2017), ε values less than 8 kJmol^{-1} shows a physical adsorption, values between 8-16 kJmol^{-1} showed a chemical adsorption and while those greater than 16 indicates particle diffusion.

Kinetics of Adsorption

Chemical kinetics deals with the experimental conditions influencing the rate of a chemical reaction. Herein, three kinetic models including the pseudo-first-order, pseudo-second-order, and intra-particle diffusion model were used to analyze the experimental data and model of the adsorption process.

Pseudo first order model

Pseudo-first order is used for adsorption in liquid-solid phase experiments. This model represents the physical adsorption of pollutants onto adsorbent surfaces (Ali, 2013). The Lagergren rate Equation of pseudo-first order is given in Equation (15) (Dada *et al.,* 2017):

$$\log(Q_e - Q_t) = \log Q_e - \frac{K_1}{2.303} t \qquad (15)$$

where Q_t is the amount of tartrazine dye adsorbed per unit of adsorbent (mg/g) at contact time t (min), Q_e is the amount of tartrazine dye adsorbed per unit mass of the adsorbent in (mg/g), k_1 is the pseudo first order rate constant (L/min). A linear plot of log (Q_e-Q_t) versus t gives k_1 as the rate constant, $-\frac{K_1}{2.303}$ as the slope, and log Q_e as the intercept (Dada *et al.,* 2017).

Blanchard pseudo-second order model

In the pseudo-second-order mechanism, the rate-limiting step is chemisorption involving covalent sharing of valency or exchange of electrons between adsorbent and adsorbate. Pseudo second-order rate equation as adopted by Rajesh *et al.,* (2014) is as presented in Equation (16):

$$\frac{t}{Q_1} = \frac{1}{K_2 Q_e^2} + \frac{1}{Q_e} t \qquad (16)$$

where K_2 is the pseudo-second order rate constant (g.mg^{-1}.min^{-1}) and the initial adsorption rate, h (mg/g.min) = $K_2 Q_e^2$. A linear plot of $\frac{t}{Q_t}$ versus t gives us K_2 the second-order Rate constant, $\frac{1}{Q_e}$ as the slope, and $\frac{1}{K_2 Q_e^2}$ as the intercept (Essomba *et al.,* 2014).

Intra-particle diffusion model

The two models above cannot identify the diffusion mechanism during the adsorption process, so the experimental data are tested by the intra-particle diffusion model, which can be expressed as equation (17):

$$Qt = kt^{0.5} + C \qquad (17)$$

where qt (mg/g) is the amount of adsorbate adsorbed at time t (min), k (mg/g min$^{1/2}$) is the intra-particle diffusion rate constant, and C is the intercept (Dada *et al.,* 2017).

Thermodynamics Studies

The spontaneity of the adsorption process is normally described by changes in the standard Gibb's free energy ($\Delta G°$) in (kJmol^{-1}), standard enthalpy change (ΔH^0) in (kJmol^{-1}) and the standard entropy change (ΔS^0) in (JK^{-1}mol^{-1}) which helps provide a better understanding of the adsorption process (Dawodu and Akpomie, 2016). The linearize form thermodynamics equation as adopted by Egah *et al.,* (2019) is given as Equation of Van't Hoff equation is given as Equation (18):

$$\log(\frac{q_e}{C_e}) = \frac{\Delta S°}{2.303R} - (\frac{\Delta H°}{2.303R})\frac{1}{T} \qquad (18)$$

where Q_e/C_e is the adsorption affinity, R is the universal gas constant (8.314 Jmol^{-1}K^{-1}), T is the temperature in (K). The thermodynamic parameters were calculated from the plot of log(qe/C_e) versus $1/T$ which gave a straight line graph where $-(\Delta H^0/2.303R)$ is the slope and ($\Delta S^0/2.303R$) is the intercept. The free Gibbs energy is given as calculated as Equation (19):

$$\Delta G° = \Delta H° - T\Delta S° \qquad (19)$$

where T is the standard temperature (298 K). If $\Delta G°$ is a negative value at a given temperature, the reaction occurs spontaneously. Adsorption is considered as exothermic reaction when $\Delta H°$ is a negative value, while it is an endothermic reaction if $\Delta H°$ is a positive value. The affinity of the adsorbent towards the adsorbate is reflected by the positive $\Delta S°$ value, suggesting the increased randomness (Al-Ghouti and Da'ana, 2020; Ashraf *et al.,* 2019).

III. RESULTS AND DISCUSSION

Physicochemical Attributes of Adsorbents

pH of the adsorbents

pH gives an idea of the acidic and basic nature of an adsorbent and is one of the most important parameters to determine the adsorption property of an adsorbent in water due to its effect on the surface charge and on the degree of ionization of adsorbate (Bousba and Meniai, 2013). From the result in Table 1, the pH of RK and KZC were found to be (6.03 and 5.12), respectively. These results are close to those obtained by Sha'Ato *et al.,* (2018) indicating slight acidic adsorbents. According to Egah *et al.,* (2023), adsorbents having neutral pH are good for adsorption. It implies that the adsorbents have a good pH for adsorption.

pHzpc of the adsorbents

pHzpc is a point of net electrical neutrality and it is used to determine the surface charge of an adsorbent which is an important indication in adsorption (Egah *et al.,* 2023). According to Makeswari *et al.,* (2016), if pHzpc > pH, the surface of the adsorbent would be positively charged, and will favour anionic adsorption. But if pH > pHzpc, the surface would be negatively charged and will favour cationic adsorption (Egah *et al.,* 2019). Results in Table 1 showed the pHzpc of the adsorbents RK and KZC to be (6.80 and 6.00) respectively. These values are higher than their corresponding pH values of (6.03 and 5.12) respectively. Indicating a positively charged adsorbent surface which favours anionic adsorption (Egah *et al.,* 2023).

Conductivity of the adsorbents

Conductivity gives an idea of the amount of charges on the surface (Sha'Ato e*t al.,* 2018). Result of Table 1, the conductivity of RK and KZC were found to be 88.30, and 68.20, at 20μS/cm respectively, indicating that the raw kaolinite RK has more surface charge than the KZC. According to a report by Sha'Ato e*t al.* (2018), high conductivity enhances the electrostatic forces between adsorbate species and adsorbent surface.

Bulk density of the adsorbents (g/cm^3)

Bulk density gives an idea of the surface area and pore volume of an adsorbent which is an important parameter in adsorbate uptake (Kibami *et al.,* 2014). Table 1, shows the bulk density values for RK and KZC to be 1.191, and 1.000, respectively. According to Egah *et al.,* (2019), low bulk density indicates high volume and large surface area for adsorption and enhances easier diffusion of adsorbates on adsorbents. From the result, KZC has a higher surface area and volume for adsorption, than the RK.

Percentage attrition of the adsorbents

Attrition is used to estimate the relative percentage loss of an adsorbent during stirring (Berez *et al*., 2014). From the results in Table 1, the percentage attrition for RK and KZC were found to be (12.00 and 12.00 %) respectively which are the same. According to Berez *et al.,* (2014), high attrition values help the adsorbents to be able to withstand Abrasion loss during utilization and therefore favor the sorption and degradation process. Similar results were obtained by Egah *et al.,* (2019) from a Synergistic Study of Hydroxyiron (III) and Kaolinite composite for the adsorptive removal of phenol and cadmium, indicating that the adsorbents are good for adsorption.

Iodine number

The iodine number is defined as the milligrams of iodine adsorbed by 1.0 g of adsorbent when the iodine concentration of the filtrate is 0.02 M (0.02 mol L^{-1}) (Nunes and Guerreiro, 2011). Results in Table 1, gave the iodine Number for the various adsorbents (RK and KZC). The iodine numbers were found to be 825.3 and 780.6 respectively. The results indicate that the iodine number of RK is greater than KZC. According to Nunes and Guerreiro (2011), the iodine number represents the number of the active site in an adsorbent. This indicates that RK has a higher iodine number than the KZC, it therefore implies they have more active sites.

Surface area, pore volume and pore size

The surface areas of the adsorbents RK and KZC were estimated using the BET as presented in Table 1. The BET surface areas (S$_{BET}$) for the adsorbents were found to be (355.744 and 385.734) m^{2}g^{-1} respectively. The pore size and pore volume were estimated using Density Functional Theory (DFT) (Thommes *et al.,* 2015). The pore volumes and pore sizes of the adsorbents were found to be (0.099 and 0.103) ccg^{-1} and (2.647 and 2.647) nm respectively. The results indicate that KZC has a greater surface area and pore volume than its corresponding RK. According to Dada *et al.,* (2017), Pores with widths exceeding 50 nm are called macropores, pores of diameters or sizes between 2 - 50 nm are called mesopores and pores diameters less than 2 nm are called micropores. This implies that both the adsorbents are mesopores. Similar results were obtained by Sodeinde *et al.,* (2021), studies on waste glass: An excellent adsorbent for crystal violet dye, Pb^{2+} and Cd^{2+} heavy metal ions decontamination from wastewater.

Table 1: Selected Physicochemical Attributes of RK and KZC

Attribute (suspension)	RK	KZC
pH (suspension)	6.03	5.12
pH$_{PZC}$ (suspension)	6.80	6.00
Conductivity (μS/cm)	88.30	68.20
Bulk-density (g/cm^3)	1.191	1.000
Attrition (%)	12.00	12.00
Iodine Number	825.3	780.6
BET Surface Area(m^2/g)	355.744	385.734

| DFT Pore volumes(cc/g) | 0.099 | 0.103 |
| DFT Pore size | 2.647 | 2.647 |

RK = Raw Kaolin; KZC = Kalinite Zinc- Oxide Composite;
BET= Brunauer-Emmett-Teller and (DFT) = Density Functional Theory

FT-IR analyses of adsorbents

The FTIR spectrum is important in the identification of surface functional groups which could play a great role in adsorption mechanism and capacity (Kibami *et al.,* 2014). According to Kibami *et al.,* (2014), good adsorbents should have specific properties such as large pores, availability of oxygen, ionizable hydrogen content, Carboxylic, and Hydroxyl groups. From the FT-IR spectrum of raw kaolinite (RK) in Figure 2, the broadband at 3690.76 cm^{-1} (ranging from 3600 – 4000 cm^{-1}) is attributed to -OH stretch from alcohols or phenols groups coordinated to octahedral Al^{3+} cations (Ahmed *et al.,* 2015). The band at 1633.33 cm^{-1} is attributed to -OH bends vibration (Faye *et al.,* 2014). The broad band at 1018.00 cm^{-1} is ascribed to the Si-O stretching vibration of silica, which agrees closely with 1027-1009cm^{-1} obtained by (Aroke *et al.,* 2013). The characteristic sharp bands at 919.79 cm^{-1} is assigned to the Al−O−H bending vibration (hydroxyl groups sitting on the alumina faces) of kaolinite (Ahmed *et al.,* 2015). The band at 759.00 cm^{-1} is attributed to Si-O stretching from silica and 686.69 cm^{-1} is attributed to -OH group symmetric stretching vibration (Liew *et al.,* 2012). The bands at 545.00 cm^{-1} and 460.29 cm^{-1} are attributed to Al-O-Si octahedral and Si-O-Si bending vibration on the raw kaolin (Moradi *et al.,* 2015). Similar results were reported by Aroke *et al.,* (2013) studies on Properties and Characterization of Kaolin Clay from Alkaleri, North-Eastern Nigeria. The FT-IR spectrum of KZC is shown in Figure 3, the bands at (3765.00, 3417.00, and 2345.55 cm^{-1}) correspond to the –OH group from alcohol at the surface of the alumina octahedral layers that interact with the oxygen atoms of the adjacent silica tetrahedral layers (Al-O-H). The band at (1629.81 cm^{-1}) is attributed to OH bend vibration (Faye *et al.,* 2014). The broad band at 1075.33 cm^{-1} is attributed to Si-O in-plane stretching vibration (Aroke *et al.,* 2013). The band at 776.62 cm^{-1} is attributed to Si-O stretching from silica and 678.66 cm^{-1} is attributed to -OH Si-O stretching vibration and O-H stretching vibration respectively (Liew *et al.,* 2012). The band at 457.86 cm^{-1} is attributed to Si-O-Si deformation (Moradi *et al.,* 2015).
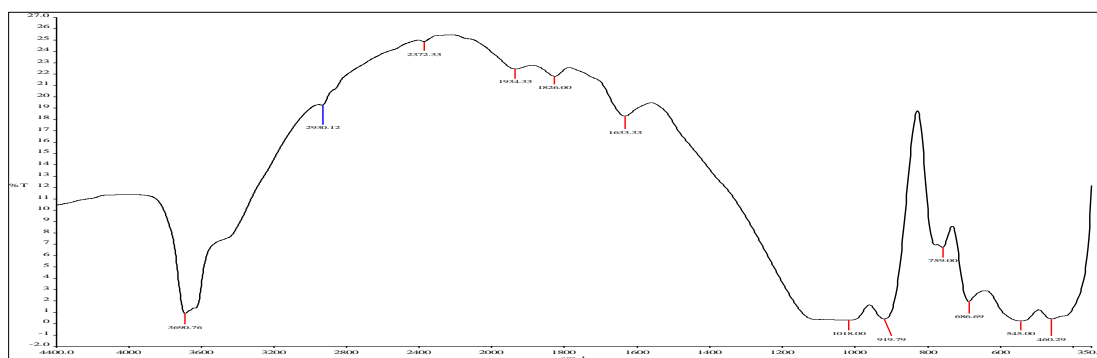

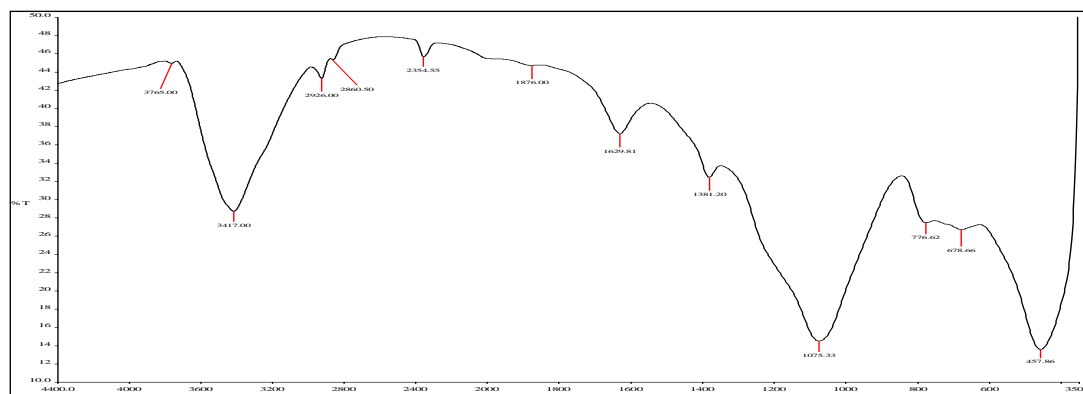**Figure 2: FTIR Spectrum of Raw Kaolinite (RK) for Adsorption**

Figure 3: FTIR Spectrum of Raw Kaolinite and Kaolinite –Zinc oxide Composites (KZC)

XRF Characterization of adsorbents

The chemical compositions of the sorbents were determined using an X-ray fluorescence instrument (XRF). This was performed using a voltage of 40 kV and 350 µA current. The chemical composition of raw kaolin RK shown in Table 2, indicates that the kaolinite sample was mainly composed of kaolinite mineral ($Al_2O_3.2SiO_2.2H_2O$) which contained SiO_2 (39.3923 %), Al_2O_3 (34.5433 %) and FeO (3.1214 %) indicating that this sample is of high grade (Ahmed *et al.,* 2015). XRF analysis of kaolinite zinc oxide composite (KZC) in Table 2 showed the percentages of ZnO (86.8218 %), WO_3 (55.3521 %), Al_2O_3 (6.0589%) and SiO_2 (5.6043 %) indicating a reduction in percentage weight which may be due to decomposition of impurities that occurred during calcination at 600 ^{o}C for 1 hr (Egah *et al.,* 2023).

Table 2: X- Ray Fluorescence Characterization of the Adsorbent

Oxide	Al_2O_3	SiO_2	K_2O	CaO	TiO_2	FeO	ZnO	WO_3	SnO_2	Sb_2O_5
RK (wt%)	34.5433	39.3923	0.2950	0.4186	1.6791	3.1214	0.3381	0.4767	2.8166	2.6725
KZC (wt)	6.0589	5.6043	0.0089	0.0418	0.0589	0.7957	86.8218	55.3521	0.1315	0.1386

Scanning electron microscopy (SEM) and EDX analyses of adsorbents

SEM results show the surface morphology feature of the adsorbents, which is an indication that an important interaction can occur between the adsorbate and adsorbent-granule interface in the experimental conditions (Egah *et al.,* 2023). Figure 4-5 shows the micrograph of RK and KZC. The raw kaolinite (RK) SEM micrograph is shown in Figure 4. The SEM micrographs indicated macro-pores with well-developed crystalline structures. The external surface shows a rough area having different irregular shapes of varying sizes and pore diameters distributed over the surface. According to El-Dars *et al.,* (2016), adsorbents with these attributes have good adsorption capacity. The EDX results in Plate 4 indicate the presence of Si, Al, and Na as major components, confirming the purity of RK material. The micrograph in Figure 5 for kaolinite zinc oxide composites (KZC), showed compact, tubular crystals and mono-disperse particle size on the surface, which increases the surface active site of the adsorbent (Ahmed *et al.,* 2015). The EDX results in Plate 5 indicate the presence of Si, Zn, Fe, and Mg as major components of KZC that aid in adsorption.
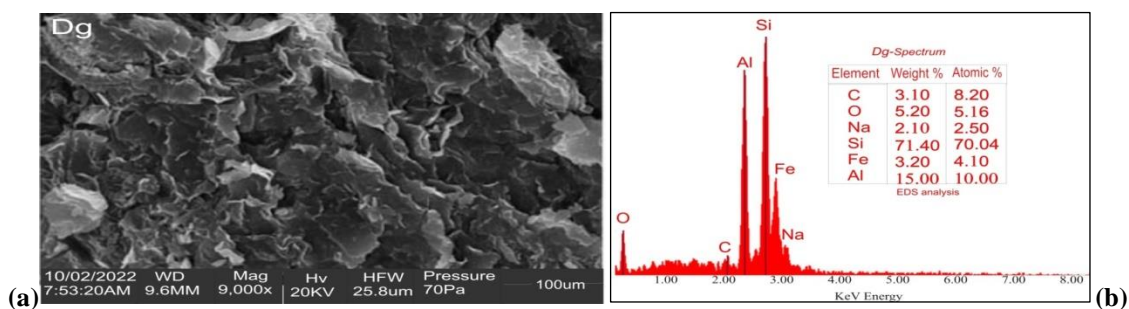

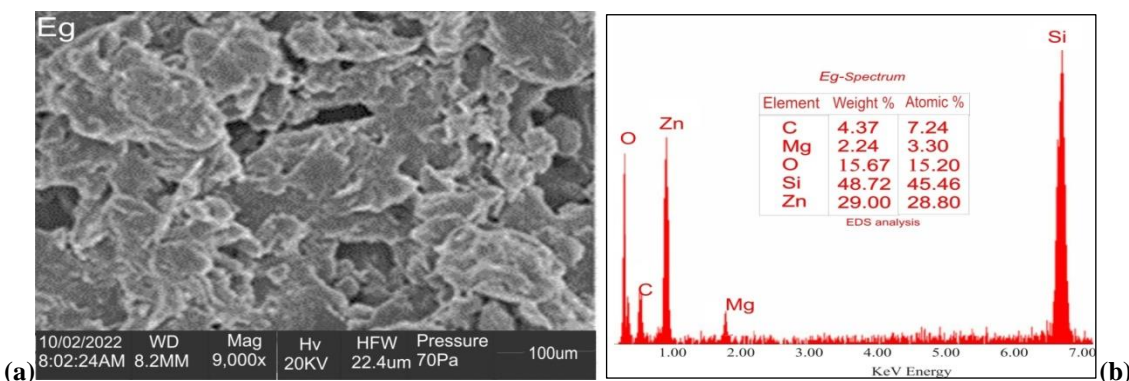**Figure 4: (a) Scanning Electron Micrograph (SEM) and (b) EDX Spectrum of RK**

Figure 5: (a) Scanning Electron Micrograph (SEM) and (b) EDX Spectrum of KZC

Effect of initial solution pH on adsorption of tartrazine

Figure 6a shows the effect of pH on the adsorption of tartrazine. From the results for the adsorbents RK and KZC, it was observed that the optimum removal was achieved at pH 3, which may be due to an increase in electrostatic attraction between the adsorbate and adsorbents (Egah *et al.,* 2023).

Effect of adsorbent dosage on tartrazine adsorption

Figure 6b shows the plot for Tartrazine removal. From the results, it was observed that as the adsorbent dosage increases from 0.5 g to 2.5 g the percentage removal increases for RK and KZC. The increasing trend in percentage removal may be attributed to the availability of the active site for adsorption which resulted in an increase in percentage removal (Sartape *et al.,* 2017). A similar trend was reported by Sartape *et al.,* (2017), a study on the removal of malachite green dye from an aqueous solution with an adsorption technique using *Limonia acidissima* (wood apple) shell as a low-cost adsorbent.

Effect of initial concentration on adsorption of tartrazine

From the results for tartrazine dye in Figure 6c, it was observed as the initial concentration of tartrazine increases from 50 – 250 mg/L that the amount adsorbed increases from 1.8866 – 10.9597 mg/g for RK and 2.1242 – 12.3672 mg/g for KZC respectively. This is an indication that at low concentrations the active sites of adsorbents are more than the available adsorbate taratrazine. Therefore, an increase in concentration leads to strong competition for adsorption sites (Bhattacharyya and Gupta, 2011; Jiang *et al.,* 2011). Under these circumstances, the unit mass of the adsorbent could take up many more tartrazine ions compared to that at lower concentrations. Similar observations for Cu (II) ions uptake on different sorbents have been reported by Bayat, (2002).

Effect of temperature on adsorption of tartrazine

From the results of tartrazine in Figure 6d, it was found that as the temperature increases from 298 -328 K, adsorption decreases from 94.6075 - 91.1409 % for RK and 96.3065 - 93.6613 % for KZC. The decrease in characteristic adsorption of tartrazine due to an increase in temperature may be due to increased randomness of the adsorbate species unavailable for the active sites of the adsorbent (Jin *et al.,* 2013). A similar result was reported by Mohanty *et al.,* (2005) study on the adsorption of phenol from aqueous solutions using activated carbons prepared from Tectona grandis sawdust by $ZnCl_2$ activation. Comparatively, from the values, it is evident that the composites KZC have a percentage removal of 96.3065 % and are more potent adsorbent than the RK with 94.6075 %. This may be attributed to their high surface charge and pore volume.

Rate curve for adsorption of tartrazine

Figure 24 shows the rate curve for tartrazine dye. From the results in Figure 6e, the highest adsorption capacity of, 8.5973 mg/g and 9.2737 mg/g was observed for RK and KZC respectively for tartrazine (10 - 60 min). Adsorption rate appeared to be very fast in the first few minutes and gradually increased to attain equilibrium at 60 minutes respectively, which could be explained due to the high number of active sights present at the starting point and as the contact time increased the active sites became saturated leading to gradual reduction as the adsorbent became saturated (Egah *et al.,* 2023). Comparatively, the removal capacity of KZC is higher than RK for the adsorbate. This suggests that they are more potent adsorbent as compared with others. The highest adsorption capacity of 4.7522 mg/g and 4.8304 mg/g were observed for RK and KZC respectively. The same trend was reported by Ahmed et al. (2015), a study on the Characterization and application of kaolinite clay as a solid phase extractor for the removal of copper ions from environmental water samples.
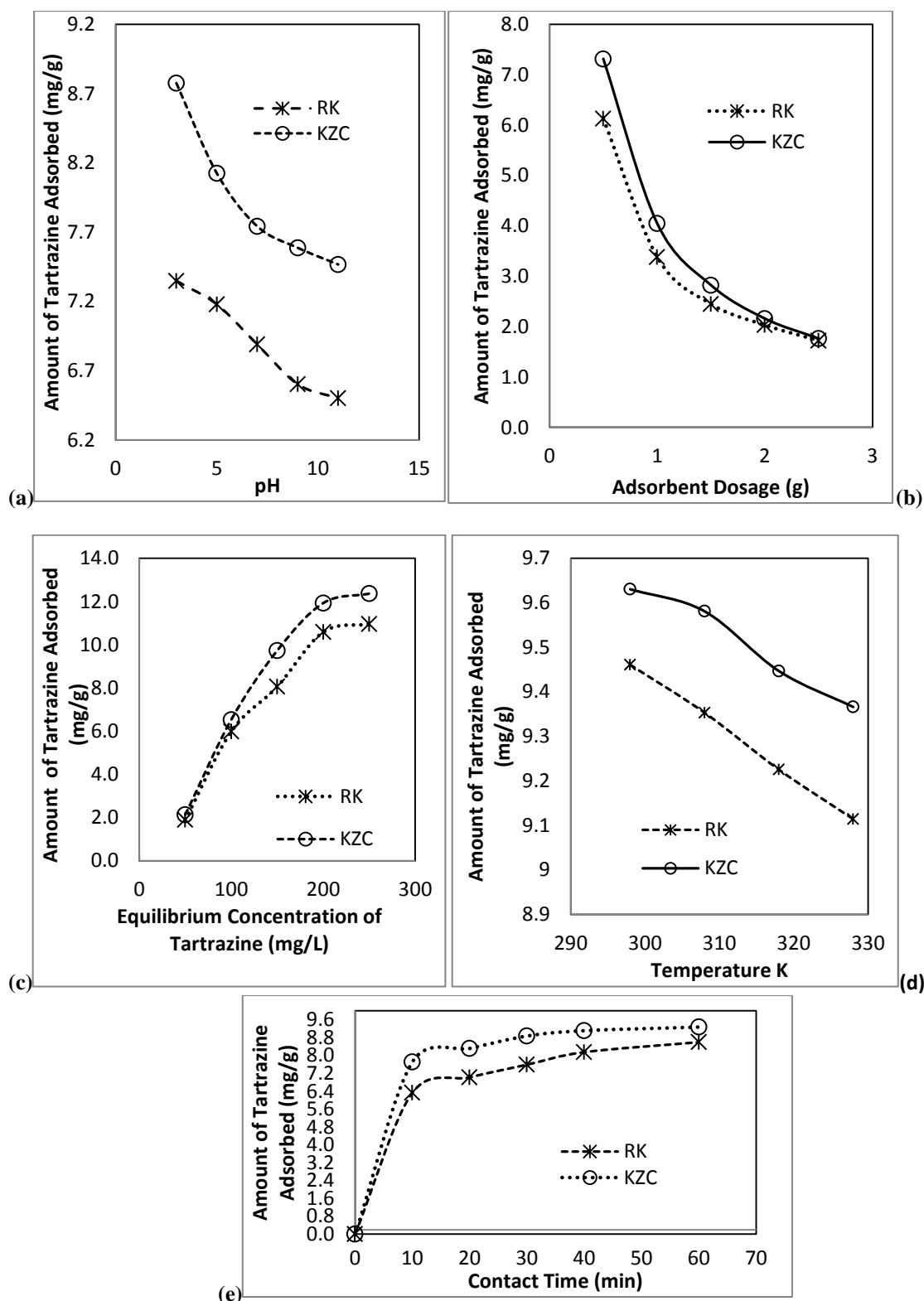
Figure 6: Effect of (a) pH, (b) Adsorbent dose, (c) Initial tartrazine concentration (d) Temperature and (e) Contact time on Aqueous Phase Removal of Tartrazine

Adsorption Kinetic Model

Data obtained from the effect of contact time on adsorption tartrazine were tested with pseudo first order, second order, and intra-particle diffusion kinetic models as presented in Table 3 Figures 7a-c. From the result for RK and KZC adsorbent, based on correlation coefficient R^2, it was observed that the Blanchard pseudo-second order for adsorption of tartrazine gave a better fitting with R^2 values of 0.9977 and 0.9998 for

RK and KZC, as compared with the Lagergren pseudo-first-order and intra particle diffusion model with values (0.4085, and 0.1003) and (0.9866 and 0.9268) for RK and KZC respectively. The high regression coefficient for the second-order shows that the pseudo-second-order equation best describes the entire adsorption process (Egah *et al.,* 2023). This implies that adsorption occurs by a chemical process involving the valence forces of exchanged electrons indicating chemisorption as the predominant rate-controlling step for the system (Sha'Ato *et al.,* 2018).
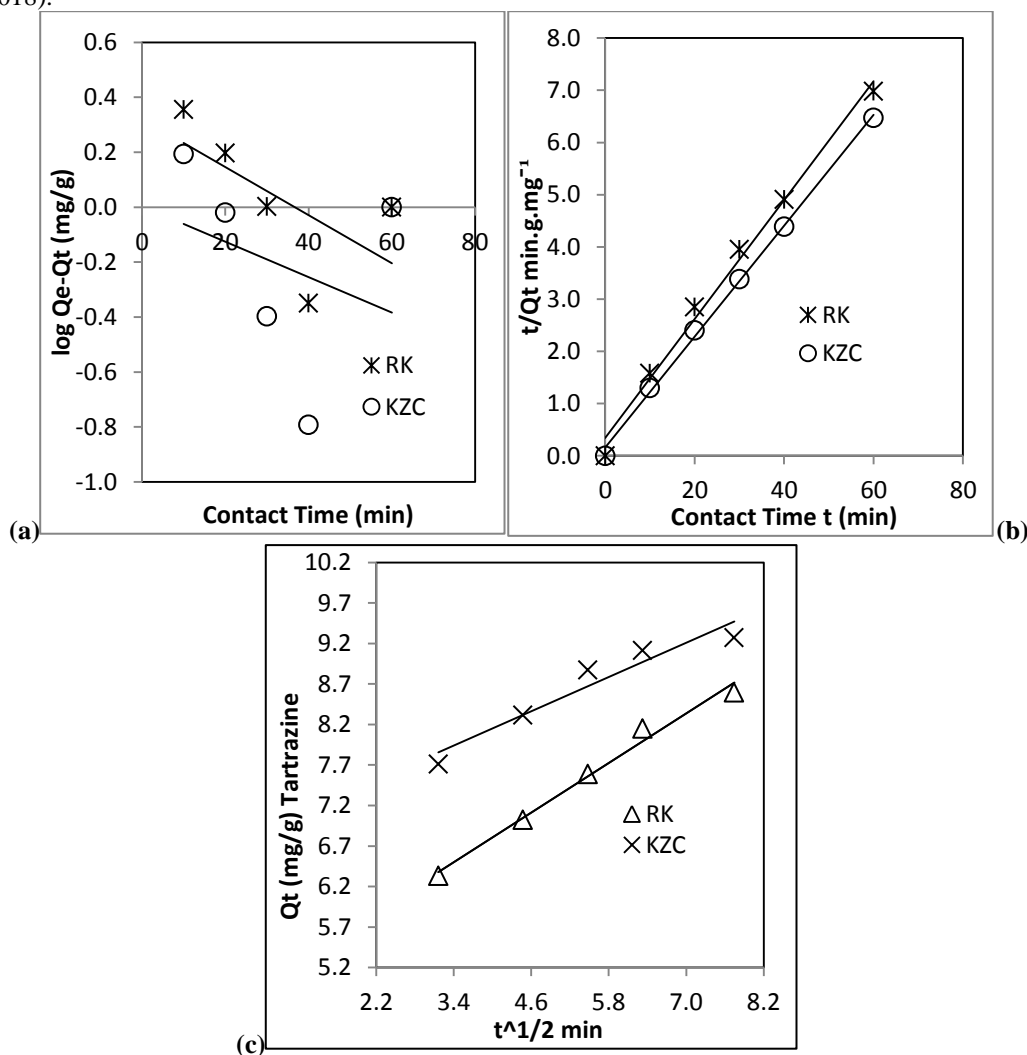

Figure 7: (a) Lagergren Pseudo-First Order, (b) Blanchard Pseudo-Second and (c) Intra Particle Difussion Kinetic Model for Removal of Tartrazine

Table 3: Kinetic Parameter for Adsorption Lagergren First Order, Blanchard Second Order and Intra Particle Diffusion Kinetic Model for Tartrazine

First order Model	RK	KZC
K_1 (Lmin^{-1})	0.0203	0.0149
Qe (mg/g)	2.0970	1.0095
R^2	0.4085	0.1003
Second order		
K_2 (g.mg^{-1}min^{-1})	0.0178	0.0353
Qe (mg/g)	9.3720	9.7276
R^2	0.9977	0.9998
h (gmg^{-1}min^{-1})	1.5630	3.3422
Intra Particle Diffusion		
K_{diff} (mg/g.min$^{1/2}$)	0.5095	0.3528
C	4.7688	6.7393
R^2	0.9866	0.9268

Adsorption Isotherm Models

The plots in Figures 8a-c and Tables 4 showed the various linearized forms of Langmuir, Freundlich, and Dubinin-Radushkevich (D-R) isotherms models. From the results in Table 4 and Figures 8a for Langmuir, the maximum adsorption capacity, Q_m for tartrazine gave values of (13.5685 mg/g and 13.8696 mg/g), for RK, and KZC respectively. These values represent, the total number of binding sites that are available for adsorption for each adsorbent (Al-Ghouti and Da'ana, 2020). The high values of KZC (13.8696 mg/g) for tartrazine is an indication that KZC has a higher number of total binding sites for adsorption of tartrazine than the corresponding RK, which may be attributed to their porosity and high conductivity (Asiagwu *et al.,* 2018). From the characteristics of the Langmuir isotherm determined from the experimental data by the dimensionless constant called separation factor, R_L, the values were all < 1 and > 0 indicating that adsorption is favourable for all adsorbents (Sartape *et al.,* 2017). From the results, the Langmuir coefficients R^2 were found to be (0.7430 and 0.6707) for RK and KZC respectively. For the results in Table 4 and Figure 8b for the Freundlich isotherm, the K_F value which is the Freundlich constant related to the adsorption capacity was found to be (0.0877 and 0.1315) (mg/g.L/mg)1/n). The regression coefficients R^2 were found to be (0.7599, and 0.6843) for RK and KZC respectively. Also results of Dubinin-Radushkevich (D-R) isotherm in Table 4 and Figure 8c, the maximum adsorption capacity of adsorbent Q_m (mg/g) were found to be 12.6835 and 15.4390 for RK and KZC respectively. The adsorption energy (ε) was found to be (40.8329 and 50.0000) kJmol^{-1} for RK and KZC respectively. According to Nwodika and Onukwuli, (2017), ε values less than 8 kJmol^{-1} show physical adsorption, values between 8-16 kJmol^{-1} show chemical adsorption, and those greater than 16 indicate particle diffusion. Since the values are greater than 16 kJmol^{-1}, it indicates particle diffusion adsorption for both RK and KZC respectively. The regression coefficients R^2 for RK and KZC were found to be 0.9385 and 0.9084 respectively. Comparing the regression coefficients R^2 for the fitness test for Langmuir, Freundlich, and D-R isotherm. The higher values for Dubinin-Radushkevich (D-R) and Freundlich isotherm suggest that the experimental data best obeyed the Dubinin-Radushkevich (D-R) and Freundlich isotherm than the Langmuir isotherm for Tartrazine. But the Dubinin-Radushkevich (D-R) model best describe the experimental data. Based on the Dubinin-Radushkevich (D-R) model, it can be concluded that the adsorption is multilayer adsorption involving Vander Waal's forces (Nwodika and Onukwuli, 2017).

Table 4: Isotherm Parameters for Tartrazine Dye Adsorption on Adsorbents

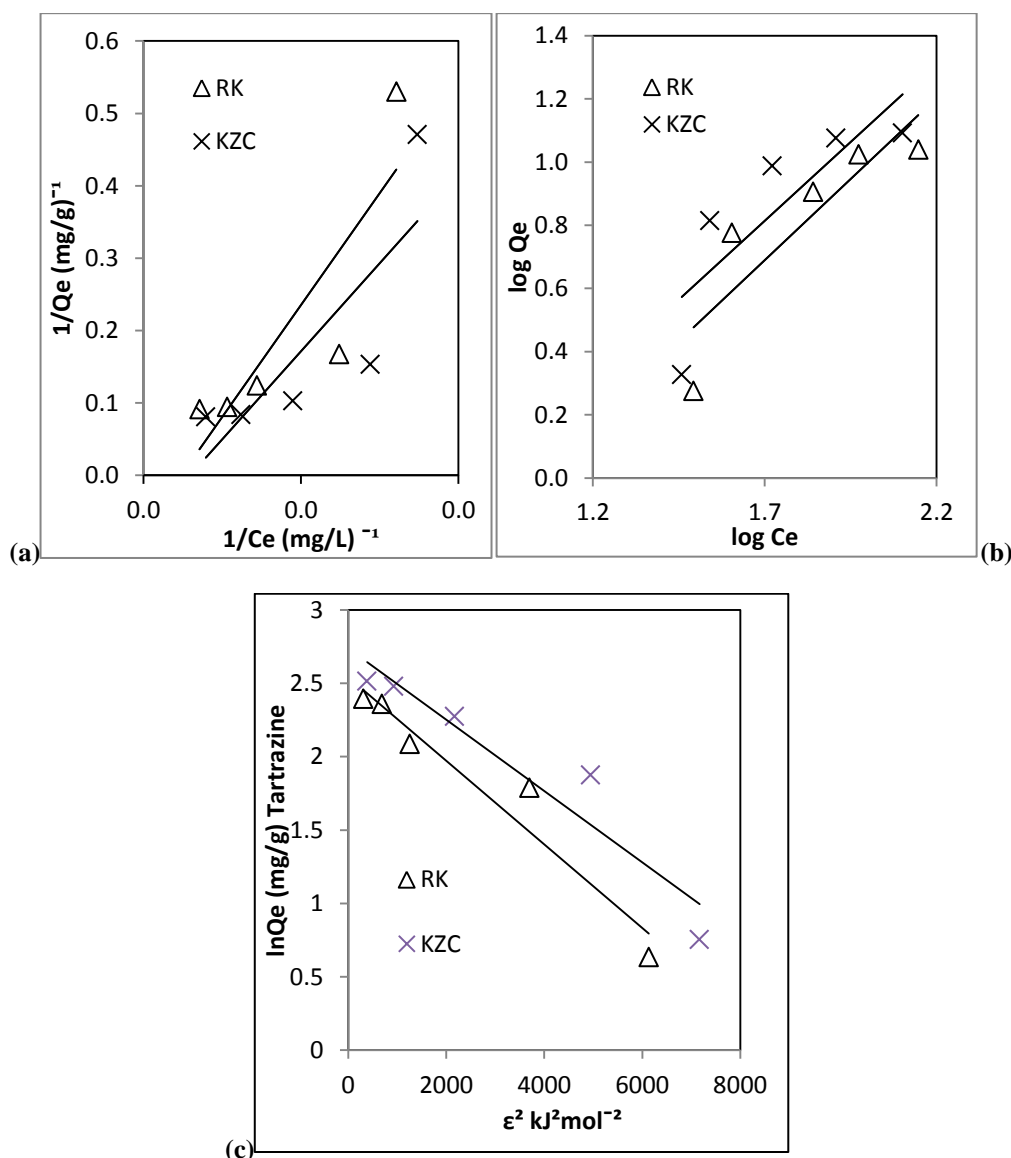| Model	RK	KZC
Langmuir		
Q_m(mg/g)	13.5685	13.8696
b (L/mg)	0.0048	0.0059
R^2	0.7430	0.6707
R_L	0.8074	0.7715
Freundlich		
1/n	1.0274	0.9971
n_F	0.9733	1.0029
R^2	0.7599	0.6843
K_F((mg/g) L/mg)1/n)	0.0877	0.1315
D-R		
Q_m, (mg/g)	12.6835	15.4390
K (mol^2/kJ^2)	3E-4	2E-4
E (kJ/mol)	40.8329	50.0000
R^2	0.9385	0.9084

(a)

(b)

(c)

Figure 8: (a)Langmuir (b) Freundlich (c) Dubinin-Radushkevich (D-R) Isotherm for Removal of Tartrazine Dye

Thermodynamic Parameters for Tartrazine Adsorption

The results in Table 5 and Figure 9 showed the calculated values of thermodynamic parameters of tartrazine on the adsorbents. From Table 5, it is observed that the values of ΔH^0 were found to be - 14.610, and - 16.207 kJmol^{-1} for RK and KZC respectively. This is an indication of the exothermic reaction of adsorption, of which physisorption dominates chemisorption (Egah *et al.,* 2023). Hence high temperature does not favour the adsorption. Similar observations and explanations have been given by Sartape *et al.,* (2017) studies on the removal of malachite green dye from an aqueous solution with an adsorption technique using *Limonia acidissima* (wood apple) shell as a low-cost adsorbent. The high negative values of ΔS^0 of (- 44.380, and - 46.208 J/molK), for RK, and KZC, are attributed to a low degree of disorder at the solid-liquid interface during adsorption processes (Tan *et al.,* 2012). The values of Gibbs free energy ΔG^0 for tartrazine were found to be (- 1.385, and - 2.437 kJ/mol) for RK and KZC respectively. These negative values suggest that the reaction is spontaneous in nature (Jameel *et al.,* 2012). Comparing the two adsorbents, the high negative values for KZC showed the feasibility of tartrazine adsorption by KZC more than the RK adsorbent (Dula *et al.,* 2014).

Table 5: Thermodynamic Parameters of Adsorption for Tartrazine

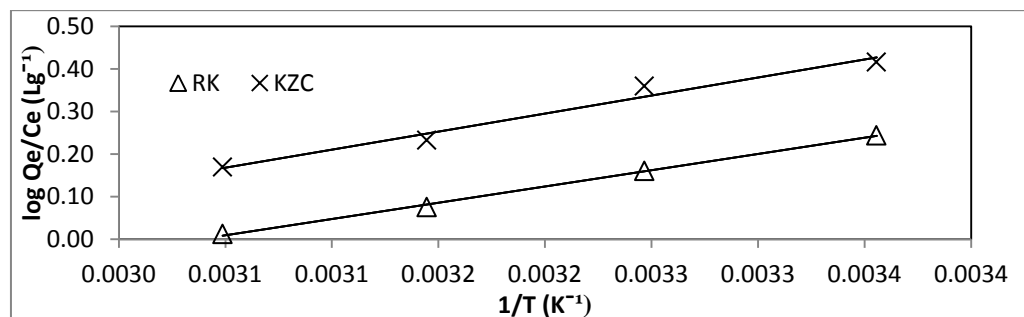| Adsorbents	ΔH(kJ/mol.1000)	ΔS(J/molK)	R²	ΔG(kJ/mol.1000)
RK	- 14.610	- 44.380	0.998	- 1.385
KZC	- 16.207	- 46.208	0.975	- 2.437

Figure 9: Van't Holf Plots for adsorption of Tartrazine

Statistical Analysis

From the ANOVA results for tartrazine at 0.05 level of significance, there is, a significant mean difference among the means of RK and KZC, since the p-value (=0.001) is less than the 0.05 level of significance. The Duncan test for tartrazine shows that the means of KZC is significantly greater than that of RK suggesting KZC composite to be more potent than RK adsorbent.

IV. CONCLUSION

From this study, it was found that the raw kaolin (RK), and Kaolinite zinc oxide composite (KZC), all exhibited good physicochemical attributes. Based on the investigation of this study, it could be concluded that the adsorption of Tartrazine dye is strongly affected by initial solution pH, initial solution concentrations, adsorbent dosage, and time of contact which favors their removal. Except for the temperature, this was found to decrease with an increase in temperature for RK and KZC. The optimum pH for adsorption of Tartrazine removal was found to be 3 respectively. For the experimental data for tartrazine, it was found that data fitted more in the linearized Dubinin-Radushkevich (D-R) and Freundlich than the Langmuir isotherm model, indicating that the adsorption is multilayer. On the effect of initial solution concentration, adsorption Tartrazine was found to increase with the increase in concentration for RK and KZC respectively. Kinetic data fitted more into the pseudo-second-order model than the first-order and intra-particle diffusion model, suggesting that physisorption dominates the rate-limiting step. All the adsorbents (RK and KZC) are capable of removing tartrazine dye solution as investigated in the present study but the KZC gave higher adsorption capacities than the RK, suggesting that the composites are more potent for the removal of tartrazine dye, which could be used for simple waste-water treatment plants in industries.

REFERENCES

[1]. Ahmed, A. S., Tantawy, A. M., Abdallah, M. E and Qassim, I. M. (2015). Characterization and application of kaolinite clay as solid phase extractor for removal of copper ions from environmental water samples, International Journal of Advanced Research, 3(3): 1-21

[2]. Al-Ghouti M. A and Da'ana D.A. (2020). Guidelines for the use and interpretation of adsorption isotherm models: A review, Journal of Hazardous Materials, 393.

[3]. Ali A. H. (2013). Comparative study on removal of cadmium (II) from simulated wastewater by adsorption onto GAC, DB, and PR, Desalination and Water Treatment, 51: 5547–5558. doi: 10.1080/19443994.2013.769927

[4]. Aroke U. O1., El-Nafaty U. A and Osha O. A(2013). Properties and Characterization of Kaolin Clay from Alkaleri, North-Eastern Nigeria. International Journal of Emerging Technology and Advanced Engineering, 3(11): 387-392.

[5]. Ashraf M.W., Abulibdeh N and Salam A. (2019).Adsorption Studies of Textile Dye (Chrysoidine) from Aqueous Solutions Using Activated Sawdust, International Journal of Chemical Engineering, 9728156: 1-8

[6]. Asiagwu, A.K., Emoyan O.O and Ojebah C.K (2018). Removal of Tartrazine Yellow Dye From Aqueous Solution using Groundnut Shell as Biomass: Kinetic Approach, International Journal of Engineering Research & Technology, 7(5): 404 – 411

[7]. ASTM International. (2014). ASTM D4607-14 standard test method for determination of iodine number of activated carbon, West Conshohocken, PA: American Society for Testing and Materials. [5 pp.].

[8]. ASTM International. (2015). ASTM C1777-15 standard test method for rapid determination of the methylene blue value for fine aggregate or mineral filler using a colorimeter, West Conshohocken, PA: American Society for Testing and Materials. [4 pp.].

[9]. Bayat, B. (2002). Comparative study of adsorption properties of Turkish fly ashes I. The case of nickel(II), copper(II) and zinc(II). Journal Hazardous Material, 95: 251–273.

[10]. Berez A., Ayari F., Abidi N., SchaFer G and Trabelsi-Ayadi, M (2014). Adsorption-desorption processes of azo dye on natural bentonite: batch experiments and modeling, Clay Minerals, 49: 747–763

[11]. Bhattacharyya, K.G and Gupta, S.S.(2011). Removal of Cu (II) by natural and acid-activated clays: an insight of adsorption isotherm, kinetics and thermodynamics. Desalination, 272: 66–75.

[12]. Bousba, S and Meniai H.A. (2013). Adsorption of 2-Chlorophenol onto Sewage Sludge based Adsorbent: Equilibrium and Kinetic Study. Chemical Engineering Transactiions, 35:859-864

[13]. Dada, A. O, Adekola F. A and Odebunmi E. O. (2017). "Kinetics, mechanism, isotherm and thermodynamic studies of liquid-phase adsorption of Pb^{2+} onto wood activated carbon supported zerovalent iron (WAC-ZVI) nanocomposite", Cogent Chemistry, (3), 1351653

[14]. Dawodu, M.O and Akpomie K.G. (2016). Evaluating the potential of a Nigerian soil as an adsorbent for tartrazine dye: Isotherm, kinetic and thermodynamic studies, Alexandria Engineering Journal, 55: 3211–3218

[15]. De Gisi, S., Lofrano G., Grassi M and Notarnicola M (2016). Characteristics and adsorption capacities of low-cost sorbents for wastewater treatment: A review, Sustainable Materials and Technologies 9: 10 – 40

[16]. Dong, Y., Wu D., Chen X and Lin Y (2010). Adsorption of bisphenol A from water by surfactant-modified zeolite, Journal of Colloid and Interface Science 348: 585–590

[17]. Dula, T., Siraj. K. and Kitte, S, A. (2014). Asdorption of hexavalent chromium from aqueous solution using chemically activated carbon prepared from locally available waste of bamboo. International scholarly Research Notices in Environmental chemistry, 2: 1-10.

[18]. Dwivedi, A. K. (2017). Researches in Water Pollution: A Review, International Research Journal of Natural and Applied Sciences, 4(1)

[19]. Egah, G. O., Hikon, B. N., Ngantem, G. S, Yerima, E. A., Omovo, M., Ogah E and Aminu, F. A. (2019). Synergistic Study of Hydroxyiron (III) and Kaolinite Composite for the Adsorptive Removal of Phenol and Cadmium. International Journal of Environmental Chemistry. 3(1): 30-42. doi: 10.11648/j.ijec.20190301.15

[20]. Egah GO; Sha'Ato R; Itodo, AU and Wuana RA (2023). Sorption of tartrazine dye from aqueous solution using activated carbon prepared from Cocos nucifera husk, International Journal of Scientific Research Updates, 06(01): 093–106

[21]. DOI: https://doi.org/10.53430/ijsru.2023.6.1.0061

[22]. El-Dars, E. S. M. F., Ibrahim, M. H., Farag, B. A. H., Abdelwahhab, Z. M and Shalabi H. E. M. (2016). Preparation, Characterization of Bentonite Carbon Composite And Design Application In Adsorption of Bromothymol Blue Dye. Journal of Multidisciplinary Engineering Science and Technology, 3(1): 3758-3765.

[23]. Essomba, S. J., Ndi Nsami, J., Belibi Belibi, B. P., Tagne, M. G and Ketcha Mbadcam, J (2014). Adsorption of Cadmium(II) Ions from Aqueous Solution onto Kaolinite and Metakaolinite. Journal, Pure and Applied Chemical Sciences, 2(1): 11 – 30

[24]. Faye G., Bekele, W and Fernandez, N. (2014). Removal of Nitrate ion from Aqueous Solution by Modified Ethiopian Bentonite Clay. International journal of research in pharmacy and chemistry, 4(1): 192-201

[25]. Huang, Z., Li, Y., Chen, W., Shi, J., Zhang, N., Wang X., Li, Z., Gao, L and Zhang, Y. (2017). Modified bentonite adsorption of organic pollutants of dye wastewater, Materials Chemistry and Physics doi: 10.1016/j.matchemphys.2017.09.028

[26]. Jameel, M. D., Hussien, A. K and Nasser, T. (2012). Removal of Cadmium Ions from Industrial Wastewater Using Iraqi Ceratophyllum Demersum. Al- Mustansiriyah Journal Science. 32(8): 71-84

[27]. Jiang, M., Jin, X., Lu, X and Chen, Z (2011). Adsorption of Pb(II), Cd(II), Ni(II) and Cu(II) onto natural kaolinite clay. Desalination, 252:33–39.

[28]. Jin, w., Hongzhu, M., Jie, Y., Shanshan, W., wenyan H, and Xiaoli, H. (2013). Studies on phenol removal from wastewater with CTAB-modified bentonite supported $KMnO_4$. Journal of Water Re-use and Desalination, 22:233-241

[29]. Johari, K., Saman, N., Song, S.T., Heng, J.Y.Y. and Mat, H. (2014). Study of Hg(II) Removal from Aqueous Solution Using Lignocellulosic Coconut Fiber Biosorbents: Equilibrium and Kinetic Evaluation Journal, 44: 1198-1220.

[30]. Karapinar, N and Donat, R. (2009). Adsorption behavior of Cu^{2+} and Cd^{2+} onto natural bentonite. Desalination, 249: 123-129.

[31]. Kibami, D., Pongener, C., K. S. Rao, K.S., and Sinha, D. (2014). Preparation and characterization of activated carbon from Fagopyrum esculentum Moench by HNO_3 and H_3PO_4 chemical activation. Der Chemica Sinica. 5(4):46-55

[32]. Liew, Y.M., Kamarudin, H., Mustafa Al Bakri, A.M., Luqman, M., KhairulNizar, I., Ruzaidi C.M. and Heah C.Y. (2012): Processing and characterization of calcined kaolin cement powder. Constructing Building Material journal, 30: 794–802.

[33]. Makeswari. M., Santhi. T and Ezhilarasi M. R. (2016). "Adsorption of methylene blue dye by citric acid modified leaves of Ricinus communis from aqueous solutions", Journal of Chemical and Pharmaceutical Research, , , 8(7):452-462

[34]. Mohanty K., Das, D., Biswas, M. N. (2005). Adsorption of phenol from aqueous solutions using activated carbons prepared from Tectona grandis sawdust by $ZnCl_2$ activation. Chemical Engineering Journal, 115(2): 121–131.

[35]. Moradi, M., Dehpahlavan, A., Kalantary, R. R., Ameri, A., Farzadkia, M and Izanloo, H. (2015). Application of modified bentonite using sulfuric acid for the removal of hexavalent chromium from aqueous solutions. Environmental Health Engineering and Management Journal, 2(3): 99–106

[36]. Naswir, M., Arita, S., Marsi and Salni. (2013). Characterization of Bentonite by XRD and SEM-EDS and Use to Increase PH and Color Removal, Fe and Organic Substances in Peat Water. Journal of Clean Energy Technologies, 1(4): 313-317.

[37]. Nunes C. A. and Guerreiro M. C.(2011). Estimation of Surface Area And Pore Volume of Activated Carbons By Methylene Blue And Iodine Numbers, Química Nova, 34(3): 472-476

[38]. Nwodika, C and Onukwuli O.C (2017). Adsorption study of kinetics and Equilibrium of Basic Dye on kola nut pod carbon, Gazi University Journal of Science, 30(4): 86-102

[39]. Okeola F. O., Odebunmi E.O., Ameen O. M., Amoloye M. A., Lawal A. A and Abdulmummeen A. G (2017). Equilibrium Kinetics and Thermodynamic Studies of the Adsorption of Tartrazine and Sunset Yellow, Arid Zone Journal of Engineering, Technology and Environment, 13(2):268-280

[40]. Pouretedal H.R and N. Sadegh (2014). Effective removal of Amoxicillin, Cephalexin, Tetracycline and Penicillin G from aqueous solutions using activated carbon nanoparticles prepared from vine wood, Journal of Water Process Engineering 1: 64–73

[41]. Prajapati, A.K and Mondal, M.K. (2020). Comprehensive kinetic and mass transfer modeling for methylene blue dye adsorption onto CuO nanoparticles loaded on nanoporous activated carbon prepared from waste coconut shell, Journal of Molecular Liquids, https://doi.org/10.1016/j.molliq.2020.112949

[42]. Rajesh, Y., Pujari, M and Uppaluri, R. (2014). Equilibrium and Kinetic Studies of Ni (II) Adsorption using Pineapple and Bamboo Stem Based Adsorbents, Separation Science and Technology, 49: 533–544

[43]. Ratna and Padhi, B.S. (2012). ''Pollution due to synthetic dyes toxicity & carcinogenicity studies and remediation'' International Journal of Environmental Sciences, 3(3).

[44]. Sartape A.S., Mandhare A.M., Jadhav V.V., Raut P.D., Anuse M.A and Kolekar S.S, (2017). Removal of malachite green dye from aqueous solution with adsorption technique using Limonia acidissima (wood apple) shell as low cost adsorbent, Arabian Journal of Chemistry, 10: S3229 –S3238

[45]. Sha'Ato, R., Egah, G.O. and Itodo, A.U. (2018). Aqueous phase abatement of phenol and cadmium using Hydroxyiron (III) calcined with bentonite. Fuw Trends in Science and Technology Journal, 3(1): 1 – 10.

[46]. Singh, J., Yadav, P., Pal, A.K. and Mishra, V. (2019). Water Pollutants: Origin and Status, Springer Nature Singapore Pte Ltd. https://doi.org/10.1007/978-981-15-0671-0_2

[47]. Sodeinde K. O., Olusanya, S. O., Momodu, D. U., Enogheghase V. F., Lawal O. S (2021): Waste glass: An excellent adsorbent for crystal violet dye, Pb^{2+} and Cd^{2+} heavy metal ions decontamination from wastewater, Journal of the Nigerian Society of Physical Sciences, 3: 414–422

[48]. Srivastav, M., Gupta, M., Agrahari, S. K and Detwal, P. (2019). Removal of Refractory Organic Compounds from Wastewater by Various Advanced Oxidation Process - A Review, Current Environmental Engineering, 6, 8-16

[49]. Tan, J., Zhang, X., Wei, X and Wang, L. (2012). Basic dye ssorption on ONP fiber. Bio-resources Journal, 7(3): 4307-4320
[50]. Thommes M., Kaneko K., Neimark A.L., Olivier J. P., Rodriguez-Reinoso F., Rouquerol J and Sing K.S.W (2015). Physisorption of gases, with special reference to the evaluation of surface area and pore size distribution (IUPAC Technical Report), Pure Applied Chemistry, 87(9-10): 1051–1069
[51]. WHO.(2008). Guidelines for Drinking-Water Quality [electronic resource]: incorporating 1st and 2nd addenda Recommendations. 3rd ed. Geneva, Switzerland, World Health Organization.